Effects of cyclic tensile strain and microgravity on the distribution of actin fiber and Fat1 cadherin in murine articular chondrocytes

Hatakeyama, Junpei ; Nomura, Masato ; Wakimoto, Yoshio ; Inoue, Shota ; Li, Changxin ; Takamura, Daisuke ; Akisue, Toshihiro ; Moriyama, Hideki

(Citation)
Journal of Biomechanics,129:110774

(Issue Date)
2021-12-02

(Resource Type)
journal article

(Version)
Accepted Manuscript

(URL)
https://hdl.handle.net/20.500.14094/90008710

Original Article

Effects of cyclic tensile strain and microgravity on the distribution of actin fiber and Fat1 cadherin in murine articular chondrocytes

Junpei Hatakeyama [a], MSc, Masato Nomura [a], MSc, Yoshio Wakimoto [a], MSc, Shota Inoue [a], MSc, Changxin Li [a], MSc, Daisuke Takamura [a, b], MSc, Toshihiro Akisue [c], MD, PhD, Hideki Moriyama [c*], PhD

[a] Department of Rehabilitation Science, Graduate School of Health Sciences, Kobe University, Tomogaoka, Suma-ku, Kobe, Japan

[b] Department of Rehabilitation, Kobe City Medical Center General Hospital, Chuo-ku, Kobe, Japan

[c] Life and Medical Sciences Area, Health Sciences Discipline, Kobe University, Tomogaoka, Suma-ku, Kobe, Japan

[*] **Correspondence:**

Hideki MORIYAMA, Ph.D.

Professor

Life and Medical Sciences Area, Health Sciences Discipline, Kobe University

Tomogaoka 7-10-2, Suma-ku, Kobe, Hyogo, 654-0142, Japan

Tel & Fax +81 78 796 4574

E-mail morihide@harbor.kobe-u.ac.jp

Key words mechanical stress, cyclic tensile strain, microgravity, actin fiber, fat1 cadherin

Words count: 3454 words

Abstract

Chondrocytes as mechano-sensitive cells can sense and respond to mechanical stress throughout life. In chondrocytes, changes of structure and morphology in the cytoskeleton have been potentially involved in various mechano-transductions such as stretch-activated ion channels, integrins, and intracellular organelles. However, the mechanism of cytoskeleton rearrangement in response to mechanical loading and unloading remains unclear. In this study, we exposed chondrocytes to a physiological range of cyclic tensile strain as mechanical loading or to simulated microgravity by 3D-clinostat that produces an unloading environment. Based on microarray profiling, we focused on Fat1 that implicated in the formation and rearrangement of actin fibers. Next, we examined the relationship between the distribution of Fat1 proteins and actin fibers after cyclic tensile strain and microgravity. As a result, Fat1 proteins did not colocalize with actin stress fibers after cyclic tensile strain, but accumulated near the cell membrane and colocalized with cortical actin fibers after microgravity. Our findings indicate that Fat1 may mediate the rearrangement of cortical actin fibers induced by mechanical unloading.

1. Introduction

Articular cartilage is daily subjected to continuous mechanical stress. Moderate mechanical loading generated by normal joint motion is essential for the maintenance of healthy articular cartilage. Meanwhile, mechanical unloading such as prolonged bed-rest (Liphardt et al., 2009) and partial load-bearing (Hinterwimmer et al., 2004) results in the reduction of cartilage thickness, which is harmful to articular cartilage. The extracellular matrix of chondrocytes allows them to withstand these changes of mechanical stress. Chondrocytes in articular cartilage are characterized by their ability to synthesize the extracellular matrix consisting of type II collagen and aggrecan (Bleuel et al., 2015). Additionally, chondrocytes as mechano-sensitive cells can sense and respond to mechanical stress (Liu et al., 2016). Despite the critical importance of mechanical loading and unloading in health and disease of articular cartilage, the mechano-transduction of chondrocytes are not fully understood.

Several studies have shown the changes of structure and morphology in the cytoskeleton are potentially involved in various mechano-transductions such as stretch-activated ion channels, integrins, and intracellular organelles (Ciccone and Med, 2016; Janmey, 1998; Salter et al., 2001). The chondrocyte cytoskeleton is composed of actin fibers, microtubules, and vimentin intermediate filaments (Langelier et al., 2000). Of these three cytoskeletons, actin fibers have been shown to be changed their structure and morphology in response to mechanical stresses. For example, compressive strain promotes the cortical actin

de-polymerization in chondrocytes (Campbell et al., 2007). Chondrocytes reorganized actin stress fibers in response to mechanical loadings such as cyclic tensile strain (CTS) (Xu et al., 2013), hydrostatic pressure (Knight et al., 2006), and compressive strain (Ofek et al., 2009). Furthermore, activation of Rho A, a member of the Rho GTPase family, was required for the formation of actin stress fibers by CTS (Sarasa-renedo et al., 2006). On the other hand, the effects of mechanical unloading on the chondrocyte cytoskeleton have been studied by simulated microgravity (μG) with parabolic flight and random positioning machines (RPM). Short parabolic flight disrupted actin fibers, and RPM changed actin fibers to be thinner and distributed to the cell membrane (Aleshcheva et al., 2015). In addition, contrary to mechanical loading, μG with RPM was contributed to the disruption of actin fibers by inactivation of Rho A (Shi et al., 2017). However, the regulation of actin fibers in response to mechanical loading and unloading is highly complex and remains unclear.

Several studies have reported that the β-tubulin (microtubules) in chondrocytes also rearranged in response to mechanical loading (Pascarelli et al., 2015; Zignego et al., 2019), however, hydrostatic stimulation did not change β-tubulin (Jortikka et al., 2000). RPM accumulated β-tubulin in the perinuclear cytoplasm after 4 hours, but did not change β-tubulin after 24 hours (Aleshcheva et al., 2013). Taken together, how β-tubulin responds to mechanical loading and unloading have been inconsistent, and therefore these mechanisms are still poorly understood.

We hypothesized that molecules identified by comprehensive gene expression analysis would be involved in the changes of actin fibers and β-tubulin after mechanical loading and unloading, leading to elucidating the mechanism of how their cytoskeleton regulates the morphology and structure through mechanical stress. In this study, we expose chondrocytes to a physiological range of CTS as mechanical loading or to a μG by 3D-clinostat that produces an unloading environment like RPM. The goal of this study was to identify how opposing loading and unloading alter gene expression implicated in the regulation of the chondrocyte cytoskeleton by microarray analysis, and to clarify the relationship between the identified potential target molecules and the cytoskeleton.

2. Materials and Methods

2.1 Experimental procedure

All experimental procedure was approved by the Institutional Animal Care and Use Committee and carried out according to the Kobe University Animal Experimentation Regulation (approval number: P140603). A total of 24 mice were used in this study. Primary articular chondrocytes were isolated from 8-weeks-old C57BL/6J mice (SLC Japan Inc., Shizuoka, Japan) as described previously (Gosset et al., 2008). Mice were intraperitoneally anesthetized with 40 mg/kg sodium pentobarbital and subcutaneously injected 0.02 mg/kg buprenorphine to give relief of pain. After dissected and removed both sides of the hindlimbs,

articular cartilage was collected from the femoral condyle and tibial plateau (knee joints from 2 or 3 mice were pooled and considered one primary chondrocyte). Articular cartilage was washed with phosphate-buffered saline (PBS) and digested with collagenase overnight. After that, cell suspension was filtered through a 100 μm cell strainer (BD Falcon, NY, USA) and centrifuged at 1200 g for 5 min. To preserve the chondrocyte phenotype, only the cells not exceeding 1 or 2 passages were adopted (Gosset et al., 2008). Cells were assigned to the following two experimental groups that were cultured under different conditions. Cells in the CTS and non-CTS control groups for CTS experiments were cultured on a collagen-coated silicone film chamber (Strex, Osaka, Japan). The other cells in the μG and normal gravity (1G) control groups for μG experiments were cultured on non-coated glass coverslips in 25 mL flasks. Cells of all groups were cultured in Dulbecco's modified Eagle's medium (D-MEM; Wako, Osaka, Japan) with 10% fetal bovine serum (Sigma Aldrich, Poole, UK), 50 μg/ml streptomycin, and 50 U/ml penicillin in an incubator set at 37℃ and supplying 5% CO_2. The media was changed once per 3 days.

2.2 CTS loading

Cells cultured in the collagen-coated silicone film chambers were stretched with STB-140 cell stretching system (Strex, Osaka, Japan). In the CTS group, CTS experiments in 8 % elongation were applied at a frequency of 0.5 Hz. Cells were continuously stretched for 48

77 hours. Cells in the non-CTS control group kept static in a CO_2 incubator without the CTS
78 loading.
79
80 2.3 μG exposure
81 μG was simulated with 3D-clinostat (PMS-VI, AES, Tokyo, Japan). 3D-clinostat generates a
82 multidirectional G force by 3D rotation. Rotational speed variances of 3D-clinostat are 0.33
83 in the X-axis, 0.34 in the Y-axis, and 0.33 in the Z-axis, which produces an unbiased
84 microgravity environment with an average of 10^{-3} G over time. The μG group were rotated
85 on 3D-clinostat in the CO_2 incubator set at 37°C for 48 hours. Cells in the 1G control group
86 were placed in the same incubator (1G).
87
88 2.4 Total RNA Isolation
89 Total RNA was isolated by ISOSPIN Cell & Tissue RNA reagent (NIPPON GENE, Tokyo,
90 Japan) according to the manufacturer's protocol. The purity and concentration of total RNA
91 were measured by BioPhotometer D30 (Eppendorf, Hamburg, Germany). Simillar to a
92 previous study (Gigante et al., 2015), total RNA with A260/280 > 1.7 and A260/A230 > 1.6
93 was used for the subsequent analysis.
94
95 2.5 Microarray analysis

For the microarray analysis, 1.0 μg of the total RNA (n = 1 per group) was amplified and labeled with Cy5 by Ambion Amino Allyl aRNA kit (Ambion, Texas, USA). Each sample of aRNA labeled with Cy5 were cohybridized with a highly sensitive DNA chip, 3D GeneTM Mouse Oligo chip 24 k (Toray Industries, Tokyo, Japan) at 37 ℃ for 16 hours. The DNA chip was then washed and dried. Hybridization signals derived from Cy5 were scanned using 3D-Gene Scanner 3000 (Toray Industries, Tokyo, Japan). Detected signals for each gene were subtracting background signal and normalized using global normalization methods (Signal value median = 25). Differentially expressed genes with fold change of $\geq \pm 1$ were used for analysis. The extracted genes were categorized into four categories. There are genes up-regulated by both CTS and μG in the Category I, genes upregulated by CTS and downregulated by μG in the Category II, genes upregulated by μG and downregulated by CTS in the Category III, and genes downregulated by both CTS and μG in the Category IV. The extracted genes were assigned to Gene Ontology (GO) Biological process by GeneCodis 4.0 databases (Carmona-saez et al., 2007).

2.6 Real-time Polymerase Chain Reaction (PCR)

To validate the microarray gene profiles, we evaluated the mRNA expression levels of Fat1 (n = 4 per group). Total RNA and the TaqMan™ Fast Virus 1-Step Master Mix (Thermo Fisher Scientific Inc., Waltham, MA, USA) were used for reverse transcription. mRNA was

115 quantitatively analyzed with the StepOne real-time polymerase chain reaction system
116 (Thermo Fisher Scientific Inc., Waltham, MA, USA) with TaqMan gene expression assays
117 (Applied Biosystems, Foster City, CA, USA) for Fat1 mRNA (Mm01200756_m1) and
118 ribosomal protein S18 rRNA (Mm03928990_g1). Fat1 mRNA expression was calculated as
119 ratios of the quantity of ribosomal protein S18 rRNA in the same cDNA sample.
120
121 2.7 Immunocytochemical staining
122 Cells were fixed with 4% paraformaldehyde in PBS for 10 min at room temperature. The
123 fixed cells were permeabilized with 0.1% Triton X-100 in PBS for 5 min and blocked with
124 10% goat serum, 1% BSA and 22.52 mg/mL glycine for 30 min. Primary antibody anti-β
125 tubulin (1:1000 dilution; ab11309; Abcam, Tokyo, Japan) or, Fat1 antibody (1:1000 dilution,
126 ab190242, Abcam, Tokyo, Japan) in 1% BSA/PBS was incubated for 2 hours at room
127 temperature. Cells were incubated with secondary antibodies anti-rabbit Alexa Fluor 555
128 (1:500 dilution; A-21429; Invitrogen, CA, USA). F-actin was stained with Acti-stain™ 488
129 phalloidin reaction solution (1:150 dilution, PHDG1-A, Cytoskeleton Inc, Denver, CO, USA)
130 for 30 min, and three washes with PBS for 5 min. Nuclei were stained with DAPI (D21490;
131 Thermo Fisher Scientific) for 1 min. After two washes with PBS, coverslips were mounted
132 with ProLong® Diamond Antifade Mountant (P36965; Invitrogen, CA, USA). Images for

chondrocytes were captured at 40× magnification. The experiment was repeated 3 times for the 1G control and μG groups, and 4 times for the non-CTS control and CTS groups.

According to the modification of a previous study (Gardner and Arnoczky, 2015), staining intensity of F-actin (n = 150-200 cells per group) and Fat1 (n = 60-70 cells per group) was measured as an indicator of their expression levels. The mean of pixel gray values (in the range 0-255) was measured after all images were converted to grayscale images using Image J 1.50 (National Institutes of Health, Bethesda, MD, USA). Additionally, the staining intensity of Fat1 in the cell cortical region (n = 60-70 cells per group) was measured as an indicator of its expression levels, referring to previous studies (Chao et al., 2006). After all images were converted to grayscale images using image J 1.50, the cell diameter was divided into six sections; and outer two regions were defined the cell cortical regions. Staining intensities of the cell cortical region were averaged and normalized to staining intensities of the whole cell region.

2. 8 Statistical analysis

The results for Fat1 mRNA expression and quantification of immunocytochemical staining were analyzed statistically using EZR (Saitama Medical Center, Jichi Medical University, Saitama, Japan), which is a graphical user interface for R (The R Foundation for Statistical Computing, Vienna, Austria). First, all values were checked for normality with the Shapiro-

Wilk test, where $P > 0.05$ indicates a normal distribution. As a result, normality was observed in all values; thus, the results were compared with Student's t-test. Comparison of all data was made between the CTS and the non-CTS groups or between the μG and the 1G groups. Significance was accepted at the 0.05 level of probability ($P < 0.05$). All values are presented as mean ± standard deviation (SD).

3. Results

3. 1 Microarray analysis of gene expression profiling

Microarray analysis revealed changes in differential expression of genes in response to CTS and μG, respectively. The CTS group upregulated 171 genes and downregulated 194 genes compared to the non-CTS control group. The μG group upregulated 112 genes and downregulated 238 genes compared to the 1G control group. To identify genes that are commonly or conflictingly affected by CTS and μG, these genes were classified into 4 categories. As shown in Fig. 1, 4 genes in Category I, 2 genes in Category II, 10 genes in Category III, and 8 genes in category IV were identified. Based on the Gene Ontology (GO) terms classification, the GO biological processes implicated in the cytoskeleton included Fat1 (GO 0007015, actin filament organization) in Category II, Fscn2 (GO 0051017, actin filament bundle formation), and Dnahc6 (GO 0007018, microtubule-based movement) in Category III (Table 1-4). In particular, Fat1 plays an important role in regulating the

171 formation and rearrangement of actin fibers (Moeller et al., 2004; Tanoue and Takeichi,
172 2004), and therefore we focused on Fat1.
173
174 3. 2 Fat1 mRNA gene expression in response to CTS and μG
175 To validate the results of microarray analysis, we quantified the expression of Fat1 mRNA
176 with real-time PCR. There were no significant differences between the CTS group and the
177 non-CTS control group (Fig. 2A). The Fat1 mRNA expression was significantly increased in
178 the μG group compared with the 1G control group (Fig. 2B). The results of Fat1 mRNA
179 expression quantified by real-time PCR were not consistent with the result of microarray
180 analysis.
181
182 3. 3 Immunocytochemical staining of β-tubulin, F-actin and Fat1
183 In all groups, β-tubulin was observed in radial morphology around the nucleus. The
184 morphology of β-tubulin was unchanged after both CTS and μG (Fig. 3A-D). F-actin of
185 chondrocytes cultured in the collagen chamber without CTS was observed in radial
186 morphology (Fig. 4A). CTS loading oriented F-actin parallel to the long axis of chondrocytes.
187 In addition, F-actin showed actin stress fibers throughout the chondrocytes (Fig. 4B). F-actin
188 of chondrocytes cultured on the glass cover with normal gravity was observed with strong
189 staining intensity (Fig. 4C). μG exposure decreased perinuclear F–actin compared to that of

the 1G control group. On the other hand, cortical F-actin was maintained after μG. (Fig, 4D). In the staining intensity of F-actin, no significant differences were found between the CTS group and the non-CTS control group (Fig. 4Q). The μG group significantly decreased the staining intensity of F-actin compared with the 1G control group (Fig. 4R). Immunocytochemical staining for Fat1 was detected in the cytoplasm, cell membrane, and nucleus of the non-CTS control group cultured in chambers on collagen (Fig. 4A, E, and M). The localization of Fat1 proteins in the CTS group was unchanged compared to the non-CTS control group. In addition, Fat1 proteins did not colocalize with actin stress fibers in the cytoplasm after CTS loading (Fig. 4B, F, and N). In the 1G control group cultured on the cover glass in the flask, Fat1 was distributed in the cytoplasm, cell membrane, and nucleus (Fig. 4C, G, and O). The μG exposure increased the accumulation of Fat1 protein near the cell membrane and colocalized Fat1 with F-actin (Fig. 4D, H, and P). The staining intensity of Fat1 in whole cell region was unchanged after both μG and CTS (Fig. 4S and T). In addition, there were no differences in the staining intensity of Fat1 in the cortical region between the CTS group and the non-CTS control group (Fig. 4U). However, the staining intensity of Fat1 in the cortical region was increased in the μG group compared with the 1G control group (Fig. 4V).

4. Discussion

209 Our objectives were to identify how CTS and μG alter gene expression implicated in the
210 regulation of the chondrocyte cytoskeleton by microarray analysis, and to clarify the
211 relationship between the identified potential target molecules and the structure of the
212 cytoskeleton. Based on microarray profiling, we identified Fat1 that implicated in the
213 formation and rearrangement of actin fibers. Next, we examined the relationship between
214 Fat1 proteins and actin fibers after CTS and μG. As a result, Fat1 proteins did not colocalize
215 with actin stress fibers after CTS loading, but accumulated in the cell membrane and
216 colocalized with cortical actin fibers after μG. These findings indicate that Fat1 may mediate
217 the formation of cortical actin fibers induced by mechanical unloading.
218 To identify genes that are commonly or conflictingly affected by CTS and μG, we
219 identify following three genes involved in the cytoskeleton: Fat1, Fscn2, and Dnahc6. Of
220 these, we focused on Fat1 because of its ability to regulate the formation and rearrangement
221 of actin fibers (Tanoue and Takeichi, 2004). This result of microarray analysis was validated
222 by real-time PCR analysis of Fat1 mRNA. Fat1 mRNA expression quantified by real-time
223 PCR was unchanged by CTS and increased by μG. These results were inconsistent with the
224 result of microarray analysis. A discrepancy between microarray analysis and real-time PCR
225 is occasionally found, e.g. due to differences in normalization methods for the target gene
226 expression (Dallas et al., 2005; Morey et al., 2006). Real-time PCR is high sensitivity,

227 accuracy, and reliability in quantifying gene expression (Mocellin et al., 2003), and therefore
228 we accepted the results of real-time PCR in this study.
229 β-tubulin, a component of microtubules, may also change its morphology in
230 response to mechanical stress such as cyclic hydrostatic compression (Pascarelli et al., 2015).
231 Contrary to this finding, the morphology of β-tubulin was unchanged when chondrocytes
232 were subjected to CTS. Our result is consistent with a previous study in which chondrocytes
233 were subjected to hydrostatic pressure (Jortikka et al., 2000). In addition, similar to a
234 previous study of RPM exposure to human chondrocytes for 24 hours (Aleshcheva et al.,
235 2013), our μG by 3D-clinostat did not change β-tubulin of chondrocytes. Taken together, our
236 results support the view that β-tubulin is not affected by mechanical loading and unloading.
237 Actin fibers organized by polymerization of monomeric G-actin change their
238 structure and morphology by mechanical stress (Halder et al., 2012). In the present study,
239 actin stress fibers in chondrocytes were observed after CTS loading. This is consistent with
240 previous studies showing the effects of CTS loading on fibroblast cells and chondrocytes
241 (Greiner et al., 2013; Xu et al., 2013). In our study, the staining intensity of F-actin as an
242 indicator of actin polymerization did not change after CTS loading. A previous study has
243 reported that CTS at the physiological intensity of 5-10% did not change actin polymerization
244 in tendon cells (Gardner and Arnoczky, 2015). Similarly, this study indicated that CTS at the
245 intensity of 8% does not change the polymerization of actin in chondrocytes. Some studies

246 have shown that RPM depolymerizes actin and disrupt actin fibers in the perinuclear
247 cytoplasm of vascular endothelial cells (Versari et al., 2007). In this study, the exposure of
248 chondrocytes to μG by 3D-clinostat decreased the staining intensity of actin fibers,
249 suggesting the depolymerization of actin. Immunocytochemical staining for F-actin in the μG
250 group showed that actin fibers in the cytoplasm were decreased, but that the cortical actin
251 fibers were maintained. Consequently, μG exposure to chondrocytes may not change the
252 structure of cortical actin fibers.

253 Fat1 cadherin proteins play an important role in regulating actin fiber formation
254 while colocalizing with actin fibers (Moeller et al., 2004; Tanoue and Takeichi, 2004).
255 PAM212 cells, which express a high level of endogenous Fat1 proteins, have been shown that
256 Fat1 proteins mainly colocalizes with cortical actin fibers (Tanoue and Takeichi, 2004). In our
257 study, Fat1 proteins did not change their expression level and localization in whole cell and
258 the cell cortical region after CTS loading. CTS loading also did not change the expression of
259 Fat1 mRNA quantified by real-time PCR. Therefore, these results suggest that Fat1 did not
260 participate in the formation of actin stress fibers by CTS loading. Meanwhile, μG
261 accumulated Fat1 proteins near the cell membrane and colocalized Fat1 proteins with cortical
262 actin fibers. Additionally, μG exposure did not change Fat1 staining intensity in whole cell
263 region, but increased in the cortical cell region. These results suggest that μG does not affect
264 the expression level of Fat1 protein per cell, but may shift the subcellular localization of Fat1

to the cortical cell. In a previous study, when Fat1 is exogenously expressed in MDCK cells, Fat1 protein was colocalized with cortical actin fiber (Tanoue and Takeichi, 2004). Therefore, an increase of Fat1 mRNA expression and Fat1 protein localized near the cell membrane may contribute to the rearrangement of cortical actin fibers after μG.

This study had several limitations. First, our study had only one experiment per group in microarray analysis as a screening. Therefore, our results of microarray analysis should be confirmed by comprehensive analysis with multiple experiments in further study. Second, in our study, chondrocytes were cultured in two different conditions. Caution should be taken with interpreting our results because the difference in substrate flexibility may potentially affect actin fiber formation (Wu et al., 1999). Finally, we only evaluated the localization of Fat1 and actin fibers. Fat1 regulates actin fiber dynamics by binding to Ena/VASP proteins through the EVH domain (Moeller et al., 2004; Tanoue and Takeichi, 2004). Further studies of Fat1 and Ena/VASP proteins are needed to clarify how Fat1 regulates actin fibers in response to μG.

In conclusion, we demonstrated that Fat1 cadherin accumulated near the cell membrane and colocalized with cortical actin fibers in chondrocytes by mechanical unloading. Given that Fat1 is required for the actin fiber formation, our findings indicate that Fat1 cadherin may mediate actin rearrangement induced by changes of mechanical stress in

chondrocytes. Future studies should assess their relationship in response to other mechanical conditions.

Conflict of Interest

All authors have no conflicts of interest.

Acknowledgements

We would acknowledge the skillful technical assistance of Mr Kosuke Watanabe. This study was supported in part by Japan Society for the Promotion of Science (JSPS) KAKENHI Grant Number 25702032.

References

Aleshcheva, G., Sahana, J., Ma, X., Hauslage, J., Hemmersbach, R., Egli, M., Infanger, M., Bauer, J., Grimm, D., 2013. Changes in morphology, gene expression and protein content in chondrocytes cultured on a random positioning machine. PLoS One 8. https://doi.org/10.1371/journal.pone.0079057

Aleshcheva, G., Wehland, M., Sahana, J., Bauer, J., Corydon, T.J., Hemmersbach, R., Frett, T., Egli, M., Infanger, M., Grosse, J., Grimm, D., 2015. Moderate alterations of the cytoskeleton in human chondrocytes after short-term microgravity produced by

parabolic flight maneuvers could be prevented by up-regulation of BMP-2 and SOX-9. FASEB J. 29, 2303–2314. https://doi.org/10.1096/fj.14-268151

Bleuel, J., Zaucke, F., Brüggemann, G.P., Niehoff, A., 2015. Effects of cyclic tensile strain on chondrocyte metabolism: A systematic review. PLoS One 10, 1–25. https://doi.org/10.1371/journal.pone.0119816

Campbell, J.J., Blain, E.J., Chowdhury, T.T., Knight, M.M., 2007. Loading alters actin dynamics and up-regulates cofilin gene expression in chondrocytes. Biochem. Biophys. Res. Commun. 361, 329–334. https://doi.org/10.1016/j.bbrc.2007.06.185

Carmona-saez, P., Chagoyen, M., Tirado, F., 2007. GENECODIS : a web-based tool for finding significant concurrent annotations in gene lists 8, 1–8. https://doi.org/10.1186/gb-2007-8-1-r3

Chao, P.H.G., West, A.C., Hung, C.T., 2006. Chondrocyte intracellular calcium, cytoskeletal organization, and gene expression responses to dynamic osmotic loading. Am. J. Physiol. - Cell Physiol. 291, 718–725. https://doi.org/10.1152/ajpcell.00127.2005

Ciccone, E., Med, J.E., 2016. Mechanotransduction Across the Cell Surface and Through the Cytoskeleton 260, 1124–1127.

Dallas, P.B., Gottardo, N.G., Firth, M.J., Beesley, A.H., Hoffmann, K., Terry, P.A., Freitas, J.R., Boag, J.M., Cummings, A.J., Kees, U.R., 2005. Gene expression levels assessed by

oligonucleotide microarray analysis and quantitative real-time RT-PCR - How well do they correlate? BMC Genomics 6, 1–10. https://doi.org/10.1186/1471-2164-6-59

Gardner, K.L., Arnoczky, S.P., 2015. High magnitude , in vitro , biaxial , cyclic tensile strain induces actin depolymerization in tendon cells Corresponding author : Muscles Ligaments Tendons J actions 3, 124–128.

Gigante, A., Bruge, F., Cecconi, S., Manzotti, S., Littarru, G.P., Tiano, L., 2015. Vitamin MK-7 enhances vitamin D3-induced osteogenesis in hMSCs: modulation of key effectors in mineralization and vascularization. J Tissue Eng Regen Med 9, 691–701. https://doi.org/10.1002/term

Gosset, M., Berenbaum, F., Thirion, S., Jacques, C., 2008. Primary culture and phenotyping of murine chondrocytes. Nat. Protoc. 3, 1253–1260. https://doi.org/10.1038/nprot.2008.95

Greiner, A.M., Chen, H., Spatz, J.P., Kemkemer, R., 2013. Cyclic Tensile Strain Controls Cell Shape and Directs Actin Stress Fiber Formation and Focal Adhesion Alignment in Spreading Cells. PLoS One 8. https://doi.org/10.1371/journal.pone.0077328

Halder, G., Dupont, S., Piccolo, S., 2012. Transduction of mechanical and cytoskeletal cues by YAP and TAZ. Nat. Rev. Mol. Cell Biol. 13, 591–600. https://doi.org/10.1038/nrm3416

Hinterwimmer, S., Krammer, M., Kro, M., Glaser, C., Baumgart, R., Reiser, M., Eckstein, F., 2004. Cartilage Atrophy in the Knees of Patients After Seven Weeks of Partial Load Bearing 50, 2516–2520. https://doi.org/10.1002/art.20378

Janmey, P.A., 1998. The cytoskeleton and cell signaling: Component localization and mechanical coupling. Physiol. Rev. 78, 763–781. https://doi.org/10.1152/physrev.1998.78.3.763

Jortikka, M.O., Parkkinen, J.J., Inkinen, R.I., Kärner, J., Järveläinen, H.T., Nelimarkka, L.O., Tammi, M.I., Lammi, M.J., 2000. The role of microtubules in the regulation of proteoglycan synthesis in chondrocytes under hydrostatic pressure. Arch. Biochem. Biophys. 374, 172–180. https://doi.org/10.1006/abbi.1999.1543

Knight, M.M., Toyoda, T., Lee, D.A., Bader, D.L., 2006. Mechanical compression and hydrostatic pressure induce reversible changes in actin cytoskeletal organisation in chondrocytes in agarose. J. Biomech. 39, 1547–1551. https://doi.org/10.1016/j.jbiomech.2005.04.006

Langelier, E., Suetterlin, R., Hoemann, C.D., Aebi, U., Buschmann, M.D., 2000. The chondrocyte cytoskeleton in mature articular cartilage: Structure and distribution of actin, tubulin, and vimentin filaments. J. Histochem. Cytochem. 48, 1307–1320. https://doi.org/10.1177/002215540004801002

356 Liphardt, A.M., Mündermann, A., Koo, S., Bäcker, N., Andriacchi, T.P., Zange, J., Mester,
357 J., Heer, M., 2009. Vibration training intervention to maintain cartilage thickness and
358 serum concentrations of cartilage oligometric matrix protein (COMP) during
359 immobilization. Osteoarthr. Cartil. 17, 1598–1603.
360 https://doi.org/10.1016/j.joca.2009.07.007
361 Liu, Q., Hu, X., Zhang, X., Duan, X., Yang, P., Zhao, F., Ao, Y., 2016. Effects of mechanical
362 stress on chondrocyte phenotype and chondrocyte extracellular matrix expression. Sci.
363 Rep. 6, 1–8. https://doi.org/10.1038/srep37268
364 Mocellin, S., Rossi, C.R., Pilati, P., Nitti, D., Marincola, F.M., 2003. Quantitative real-time
365 PCR: A powerful ally in cancer research. Trends Mol. Med. 9, 189–195.
366 https://doi.org/10.1016/S1471-4914(03)00047-9
367 Moeller, M.J., Soofi, A., Braun, G.S., Li, X., Watzl, G., Kriz, W., Holzman, L.B., 2004.
368 Protocadherin FAT1 binds Ena/VASP proteins and is necessary for actin dynamics and
369 cell polarization. EMBO J. 23, 3769–3779. https://doi.org/10.1038/sj.emboj.7600380
370 Morey, J.S., Ryan, J.C., Van Dolah, F.M., 2006. Microarray validation: Factors influencing
371 correlation between oligonucleotide microarrays and real-time PCR. Biol. Proced.
372 Online 8, 175–193. https://doi.org/10.1251/bpo126

373 Ofek, G., Wiltz, D.C., Athanasiou, K.A., 2009. Contribution of the cytoskeleton to the
374 compressive properties and recovery behavior of single cells. Biophys. J. 97, 1873–
375 1882. https://doi.org/10.1016/j.bpj.2009.07.050
376 Pascarelli, N.A., Collodel, G., Moretti, E., Cheleschi, S., Fioravanti, A., 2015. Changes in
377 ultrastructure and cytoskeletal aspects of human normal and osteoarthritic chondrocytes
378 exposed to interleukin-1β and cyclical hydrostatic pressure. Int. J. Mol. Sci. 16, 26019–
379 26034. https://doi.org/10.3390/ijms161125936
380 Salter, D.M., Millward-Sadler, S.J., Nuki, G., Wright, M.O., 2001. Integrin-interleukin-4
381 mechanotransduction pathways in human chondrocytes. Clin. Orthop. Relat. Res. 49–60.
382 https://doi.org/10.1097/00003086-200110001-00006
383 Sarasa-renedo, A., Tunç-civelek, V., Chiquet, M., 2006. Role of RhoA / ROCK-dependent
384 actin contractility in the induction of tenascin-C by cyclic tensile strain 2.
385 https://doi.org/10.1016/j.yexcr.2005.12.025
386 Shi, F., Wang, Y.C., Hu, Z.B., Xu, H.Y., Sun, J., Gao, Y., Li, X.T., Yang, C. Bin, Xie, C., Li,
387 C.F., Zhao, J.D., Zhang, S., Cao, X.S., Sun, X.Q., 2017. Simulated microgravity
388 promotes angiogenesis through rhoa-dependent rearrangement of the actin cytoskeleton.
389 Cell. Physiol. Biochem. 41, 227–238. https://doi.org/10.1159/000456060
390 Tanoue, T., Takeichi, M., 2004. Mammalian Fat1 cadherin regulates actin dynamics and cell-
391 cell contact. J. Cell Biol. 165, 517–528. https://doi.org/10.1083/jcb.200403006

Versari, S., Villa, A., Bradamante, S., Maier, J.A.M., 2007. Alterations of the actin cytoskeleton and increased nitric oxide synthesis are common features in human primary endothelial cell response to changes in gravity. Biochim. Biophys. Acta - Mol. Cell Res. 1773, 1645–1652. https://doi.org/10.1016/j.bbamcr.2007.05.014

Wu, Z., Wong, K., Glogauer, M., Ellen, R.P., McCulloch, C.A.G., 1999. Regulation of stretch-activated intracellular calcium transients by actin filaments. Biochem. Biophys. Res. Commun. 261, 419–425. https://doi.org/10.1006/bbrc.1999.1057

Xu, T., Yang, K., You, H., Chen, A., Wang, J., Xu, K., Gong, C., Shao, J., Ma, Z., Guo, F., Qi, J., 2013. Regulation of PTHrP expression by cyclic mechanical strain in postnatal growth plate chondrocytes. Bone 56, 304–311. https://doi.org/10.1016/j.bone.2013.06.027

Zignego, D.L., Hilmer, J.K., Bothner, B., Schell, W.J., June, R.K., 2019. Primary human chondrocytes respond to compression with phosphoproteomic signatures that include microtubule activation. J. Biomech. 97, 109367. https://doi.org/10.1016/j.jbiomech.2019.109367

Figure Legends

Fig. 1. Microarray analysis of gene expression profiling

Microarray profiling of chondrocytes showed genes that are commonly or conflictingly regulated by CTS and μG (n = 1 per group). Category I: genes upregulated by both CTS and μG, Category II: genes upregulated by CTS and downregulated by μG, Category III: genes upregulated by μG and downregulated by CTS, and Category VI: genes downregulated by both CTS and μG.

Fig. 2. Fat1 mRNA gene expression in response to CTS and μG

The graphs show the expression of Fat1 in each group. Data are shown as the mean ± SD of 4 wells per group. *$P < 0.05$.

Fig. 3. Immunocytochemical staining of β-tubulin

Representative images of immunocytochemical staining shows (A-D) β-tubulin.in each group Scale bars = 50 μm.

Fig. 4. Immunocytochemical staining of F-actin and Fat1

Representative images of immunocytochemical staining shows (A-B) F-actin, (E-H) Fat1, (I-L) nucleus staining-DAPI, and (M-P) Merge in each group. Scale bars = 50 μm. The graph

right shows staining intensity of (Q and R) F-Actin in whole cell region (n =150-200 cells per group), (S and T) Fat1 in whole cell region (n = 60-70 cells per group), and (U and V) Fat1 in the cell cortical region (n =60-70 cells per group) in each group. Data are shown as the mean ± SD. *$P < 0.05$.

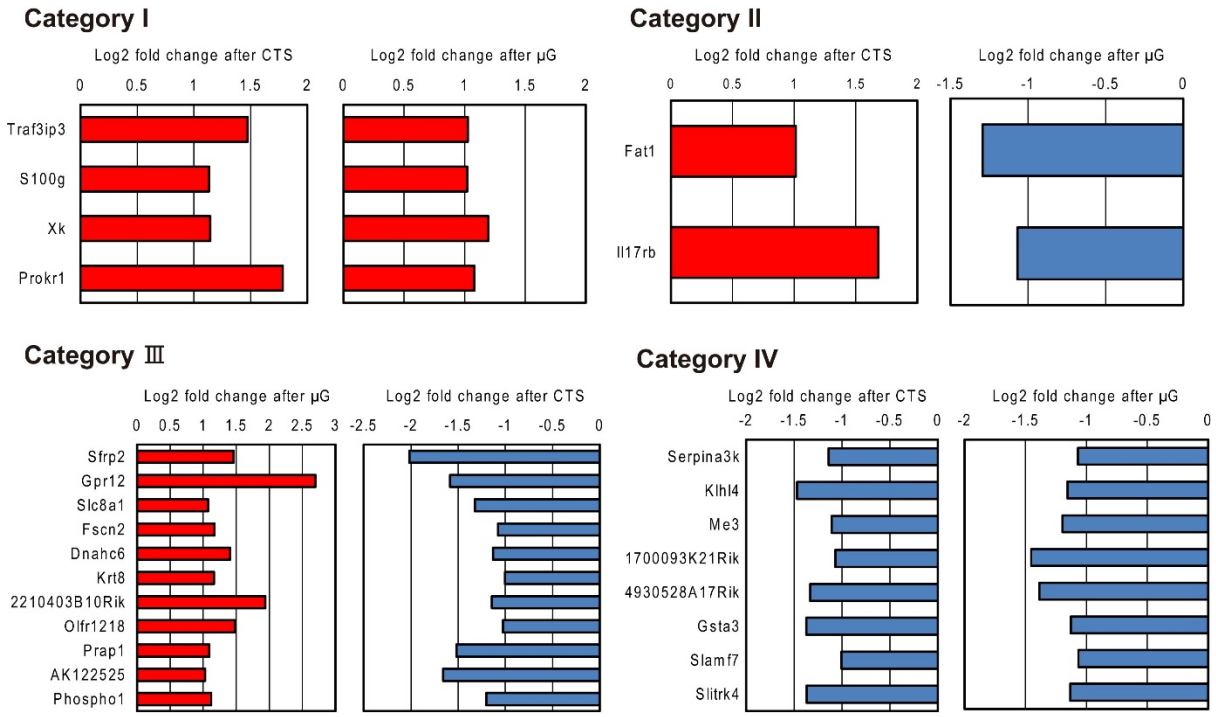
Category I
Log2 fold change after CTS
Log2 fold change after μG
0 0.5 1 1.5 2
Traf3ip3
S100g
Xk
Prokr1
Category II
Log2 fold change after CTS
Log2 fold change after μG
0 0.5 1 1.5 2
-1.5 -1 -0.5 0
Fat1
Il17rb
Category Ⅲ
Log2 fold change after μG
Log2 fold change after CTS
0 0.5 1 1.5 2 2.5 3
-2.5 -2 -1.5 -1 -0.5 0
Sfrp2
Gpr12
Slc8a1
Fscn2
Dnahc6
Krt8
2210403B10Rik
Olfr1218
Prap1
AK122525
Phospho1
Category IV
Log2 fold change after CTS
Log2 fold change after μG
-2 -1.5 -1 -0.5 0
Serpina3k
Klhl4
Me3
1700093K21Rik
4930528A17Rik
Gsta3
Slamf7
Slitrk4

Figure 1

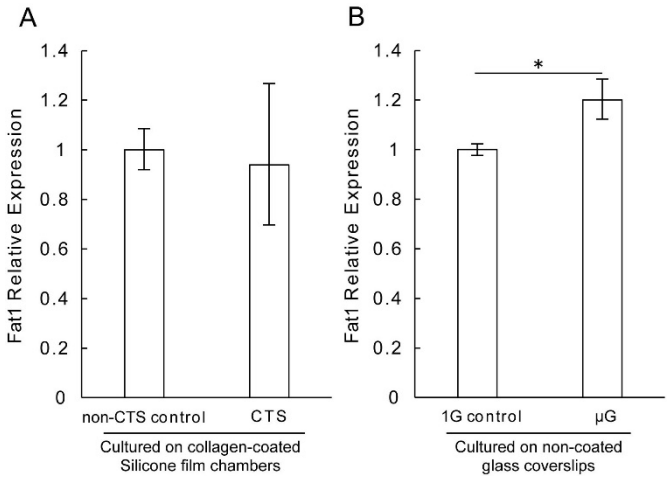
A
B
Fat1 Relative Expression
1.4
1.2
1
0.8
0.6
0.4
0.2
0
non-CTS control
CTS
Cultured on collagen-coated
Silicone film chambers
*
1G control
μG
Cultured on non-coated
glass coverslips

Figure 2

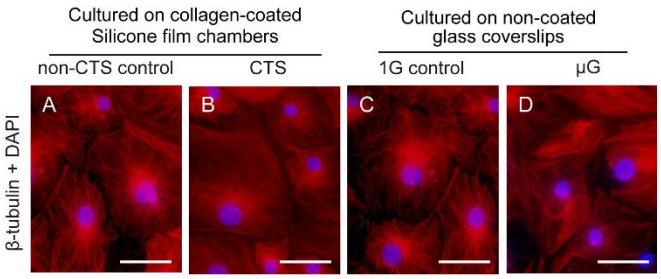
Cultured on collagen-coated
Silicone film chambers
Cultured on non-coated
glass coverslips
non-CTS control
CTS
1G control
μG
A
B
C
D
β-tubulin + DAPI

Figure 3

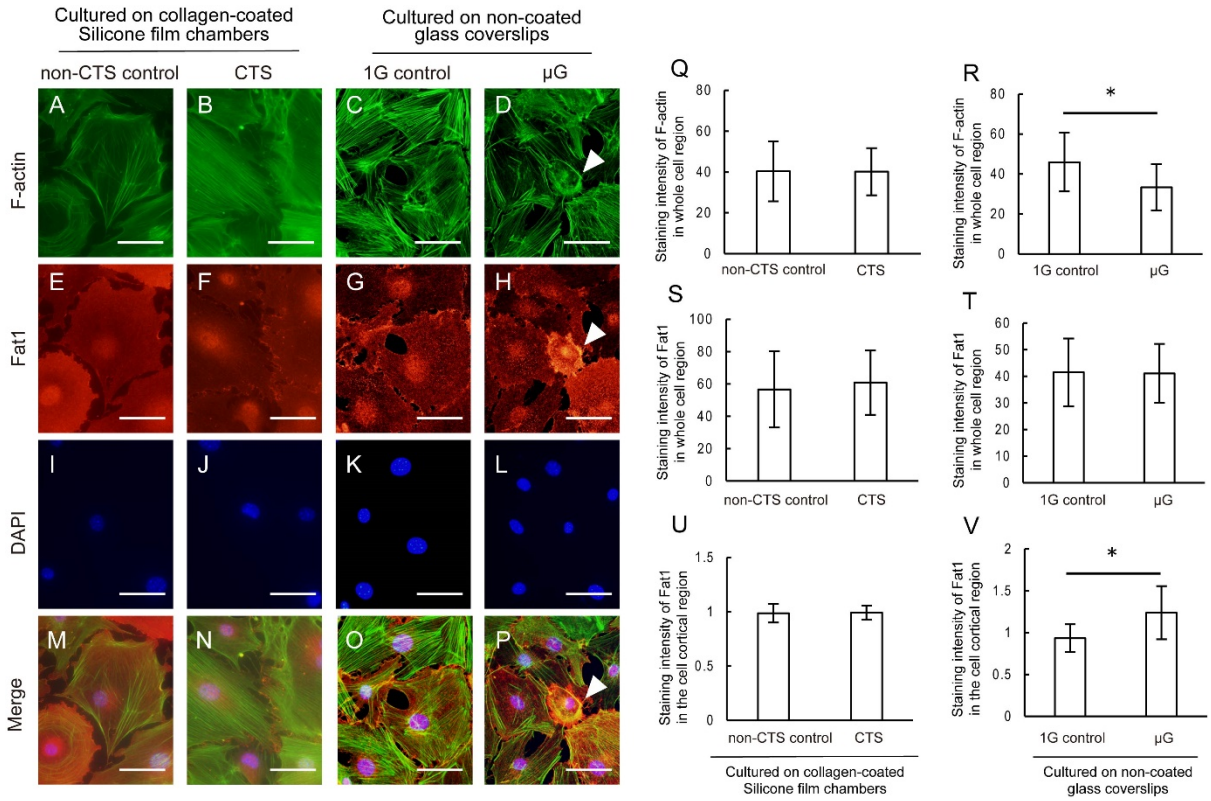
Cultured on collagen-coated Silicone film chambers
Cultured on non-coated glass coverslips
non-CTS control
CTS
1G control
μG
F-actin
Fat1
DAPI
Merge
A
B
C
D
E
F
G
H
I
J
K
L
M
N
O
P
Q
R
S
T
U
V
Staining intensity of F-actin in whole cell region
Staining intensity of Fat1 in whole cell region
Staining intensity of Fat1 in the cell cortical region
*
Cultured on collagen-coated Silicone film chambers
Cultured on non-coated glass coverslips

Figure 4

Table 1. GO terms of genes upregulated by both CTS and μG

symbol	description	GO biological process
Traf3ip3	TRAF3 interacting protein 3	GO:0008150 (biological process)
S100g	S100 calcium binding protein G	Unavailable annotation
Xk	Kell blood group precursor (McLeod phenotype) homolog	GO:0006865 (amino acid transport) GO:0006874 (cellular calcium ion homeostasis) GO:0008361 (regulation of cell size) GO:0010961 (cellular magnesium ion homeostasis) GO:0042552 (myelination) GO:0048741 (skeletal muscle fiber development)
Prokr1	prokineticin receptor 1	GO:0007165 (signal transduction) GO:0007186 (G-protein coupled receptor protein signaling pathway) GO:0007623 (circadian rhythm) GO:0043066 (negative regulation of apoptotic process) GO:0060976 (coronary vasculature development)

Table 2. GO terms of genes upregulated by CTS and downregulated by μG

symbol	description	GO biological process
Fat1	FAT tumor suppressor homolog 1	GO:0002088 (lens development in camera-type eye) GO:0003382 (epithelial cell morphogenesis) GO:0003412 (establishment of epithelial cell apical/basal polarity involved in camera-type eye morphogenesis) GO: 0007015（actin filament organization） GO:0007155 (cell adhesion) GO: 0007156（homophilic cell adhesion via plasma membrane adhesion molecules） GO: 0007163 (establishment and/or maintenance of cell polarity) GO: 0016337 (cell-cell adhesion) GO:0043010 (camera-type eye development) GO:0045197 (establishment or maintenance of epithelial cell apical/basal polarity) GO:0048593 (camera-type eye morphogenesis) GO:0050729 (positive regulation of inflammatory response) GO:0098609 (cell-cell adhesion)
Il17rb	interleukin 17 receptor B	GO:0019221 (cytokine-mediated signaling pathway cytokine-mediated signaling pathway) GO:0032736 (positive regulation of interleukin-13 production) GO:0032754 (positive regulation of interleukin-5 production) GO:0050729 (positive regulation of inflammatory response)

Table 3. GO terms of genes upregulated by μG and downregulated by CTS

symbol	description	GO biological process
Sfrp2	secreted frizzled-related protein 2	GO:0001569 (branching involved in blood vessel morphogenesis) GO:0001756 (somitogenesis) GO:0002063 (chondrocyte development) GO:0003214 (cardiac left ventricle morphogenesis) GO:0007584 (response to nutrient) GO:0010975 (regulation of neuron projection development) GO:0010719 (negative regulation of epithelial to mesenchymal transition) GO:0010667 (negative regulation of cardiac muscle cell apoptotic process) GO:0010950 (positive regulation of endopeptidase activity) GO:0021915 (neural tube development) GO:0030111 (regulation of Wnt signaling pathway) GO:0030178 (negative regulation of Wnt signaling pathway) GO:0030199 (collagen fibril organization) GO:0030514 (negative regulation of BMP signaling pathway) GO:0003151 (outflow tract morphogenesis) GO:0031668 (cellular response to extracellular stimulus) GO:0035567 (non-canonical Wnt signaling pathway) GO:0036342 (post-anal tail morphogenesis) GO:0042493 (response to drug) GO:0042733 (embryonic digit morphogenesis)

		GO:0045600 (positive regulation of fat cell differentiation) GO:0042662 (negative regulation of mesodermal cell fate specification) GO:0043508 (negative regulation of JUN kinase activity) GO:0046546 (development of primary male sexual characteristics) GO:0048546 (digestive tract morphogenesis) GO:0050732 (negative regulation of peptidyl-tyrosine phosphorylation) GO:0060028 (convergent extension involved in axis elongation) GO:0060349 (bone morphogenesis) GO:0061056 (sclerotome development) GO:0061185 (negative regulation of dermatome development) GO:0071425 (hematopoietic stem cell proliferation) GO:0071481 (cellular response to X-ray) GO:0090175 (regulation of establishment of planar polarity) GO:0090179 (planar cell polarity pathway involved in neural tube closure) GO:0090244 (Wnt signaling pathway involved in somitogenesis) GO:1902042 (negative regulation of extrinsic apoptotic signaling pathway via death domain receptors) GO:1904956 (regulation of midbrain dopaminergic neuron differentiation) GO:2000035 (regulation of stem cell division) GO:2000041 (negative regulation of planar cell polarity pathway involved in axis elongation)
Gpr12	G-protein coupled receptor 12	GO:0006874 (calcium ion homeostasis) GO:0007165 (signal transduction) GO:0007186 (G-protein coupled receptor protein signaling pathway)

		GO:0019222 (regulation of metabolic process)
Slc8a1	solute carrier family 8 (sodium/calcium exchanger), member 1	GO:0001892 (embryonic placenta development) GO:0002026 (regulation of the force of heart contraction) GO:0002027 (regulation of heart rate) GO:0002028 (regulation of sodium ion transport) GO:0006874 (cellular calcium ion homeostasis) GO:0006883 (cellular sodium ion homeostasis) GO:0007154 (cell communication) GO:0007584 (response to nutrient) GO:0010763 (positive regulation of fibroblast migration) GO:0010881 (regulation of cardiac muscle contraction by regulation of the release of sequestered calcium ion) GO:0014829 (vascular associated smooth muscle contraction) GO:0021537 (telencephalon development) GO:0030001 (metal ion transport) GO:0030501 (positive regulation of bone mineralization) GO:0033198 (response to ATP) GO:0034614 (cellular response to reactive oxygen species) GO:0035050 (embryonic heart tube development) GO:0035902 (response to immobilization stress) GO:0035994 (response to muscle stretch) GO:0036376 (sodium ion export across plasma membrane) GO:0042493 (response to drug) GO:0042542 (response to hydrogen peroxide)

GO:0044557 (relaxation of smooth muscle)
GO:0048747 (muscle fiber development)
GO:0051481 (negative regulation of cytosolic calcium ion concentration)
GO:0051924 (regulation of calcium ion transport)
GO:0055013 (cardiac muscle cell development)
GO:0055074 (calcium ion homeostasis)
GO:0060048 (cardiac muscle contraction)
GO:0060402 (calcium ion transport into cytosol)
GO:0070509 (calcium ion import)
GO:0071313 (cellular response to caffeine)
GO:0071320 (cellular response to cAMP)
GO:0071901 (negative regulation of protein serine/threonine kinase activity)
GO:0086036 (regulation of cardiac muscle cell membrane potential)
GO:0086064 (cell communication by electrical coupling involved in cardiac conduction)
GO:0098703 (calcium ion import across plasma membrane)
GO:0098719 (sodium ion import across plasma membrane)
GO:0098735 (positive regulation of the force of heart contraction)
GO:0099566 (regulation of postsynaptic cytosolic calcium ion concentration)
GO:1901660 (calcium ion export)

Fscn2	fascin homolog 2, actin-bundling protein, retinal	GO:0007163 (establishment or maintenance of cell polarity) GO:0042462 (eye photoreceptor cell development) GO:0051017(actin filament bundle assembly)
Dnahc6	dynein, axonemal, heavy chain 6	GO:0003341 (cilium movement) GO:0007018(microtubule-based movement) GO:0060285 (cilium-dependent cell motility)
Krt8	keratin 8	GO:0000904 (cell morphogenesis involved in differentiation) GO:0033209 (tumor necrosis factor-mediated signaling pathway) GO:0045214 (sarcomere organization) GO:0051599 (response to hydrostatic pressure) GO:0051707 (response to other organism) GO:0060706 (cell differentiation involved in embryonic placenta development) GO:0097191 (extrinsic apoptotic signaling pathway) GO:0097284 (hepatocyte apoptotic process)
2210403B10Rik	RIKEN cDNA 2210403B10 gene	GO:0007165 (signal transduction)
Olfr1218	olfactory receptor 1218	GO:0007165 (signal transduction) GO:0007186 (G-protein coupled receptor protein signaling pathway) GO:0007608 (sensory perception of smell) GO:0050911 (detection of chemical stimulus involved in sensory perception of smell)
Prap1	proline-rich acidic protein 1	Unavailable annotation

AK122525	cDNA sequence AK122525	Unavailable annotation
Phospho1	phosphatase, orphan 1	GO:0001958 (endochondral ossification) GO:0030500 (regulation of bone mineralization) GO:0035630 (bone mineralization involved in bone maturation)

Table 4. GO terms of genes downregulated by both CTS and μG

symbol	description	GO biological process
Serpina3k	serine (or cysteine) peptidase inhibitor, clade A, member 3K	GO:0010466 (negative regulation of peptidase activity) GO:0010951 (negative regulation of endopeptidase activity) GO:0034097 (response to cytokine) GO:0043434 (response to peptide hormone)
Klhl4	kelch-like 4 (Drosophila)	GO:0008150 (biological_process)
Me3	malic enzyme 3, NADP(+)-dependent, mitochondrial	GO:0006090(pyruvate metabolic process) GO:0006108(malate metabolic process)
1700093K21Rik	RIKEN cDNA 1700093K21 gene	GO:0008150 (biological_process)
4930528A17Rik	RIKEN cDNA 4930528A17 gene	Unavailable annotation
Gsta3	glutathione S-transferase, alpha 3	GO:0001657 (ureteric bud development) GO:0006749 (glutathione metabolic process) GO:0006805 (xenobiotic metabolic process) GO:0046223 (aflatoxin catabolic process)
Slamf7	SLAM family member 7	GO:0002250 (adaptive immune response) GO:0032814 (regulation of natural killer cell activation) GO:0045087 (innate immune response)
Slitrk4	SLIT and NTRK-like family, member 4	GO:0007409 (axonogenesis) GO:0050807 (egulation of synapse organization) GO:0051965 (positive regulation of synapse assembly) GO:1905606 (regulation of presynapse assembly)